^{43}K(β^-)^{43}Ca and the structure of ^{43}K and ^{43}Ca

E. K. Warburton and D. E. Alburger
Brookhaven National Laboratory, Upton, New York 11973
(Received 12 August 1988)

The β^- decay of 22 h ^{43}K ($J^\pi=\frac{3}{2}^+$) was reexamined with the main motive of determining the first-forbidden β^- branches to the $\frac{3}{2}^-$ and $\frac{5}{2}^-$ states more accurately. The branch to the $\frac{5}{2}^-$ state at 373 keV was established as 0.9(6)% as opposed to a previous limit of <3%. Other β^- and γ branching ratios and γ-ray energies were determined with considerably improved accuracy. Shell-model calculations in full $(2s,1d)^{24}(1f,2p)^3$ and $(2s,1d)^{23}(1f,2p)^4$ configurational spaces were carried out using the WBMB spherical shell-model interaction. Energy spectra, nucleon pickup spectroscopic factors from ^{44}Ca, two-nucleon transfer strengths from ^{41}K, and γ-ray transition rates were calculated for both ^{43}K and ^{43}Ca as well as allowed and first-forbidden decays for the known branches in ^{43}K(β^-) ^{43}Ca. Results are compared to experiment.

I. INTRODUCTION

Our interest in the spectroscopy of ^{43}K-^{43}Ca is motivated by two factors. First, current interest in first-forbidden beta transitions ($\Delta J\leq 2, \pi_i\pi_f=-$) and, in particular, the mesonic enhancement of $\Delta J=0$ transitions,[1-7] and second, the desire to utilize the cross-shell spherical shell-model interaction WBMB (Refs. 7–9) in as heavy a system as possible.

The $\frac{3}{2}^+$ ^{43}K ground state arises primarily from the shell-model configuration $(2s,1d)^{23}(1f,2p)^4$ outside an inert ^{16}O core and its decay by β^- emission is primarily to the fourth and fifth states of ^{43}Ca, both of even parity, which are presumably of the same configuration. The first three states of ^{43}Ca are all of odd parity and presumably arise primarily from $(1f,2p)^3$ outside an inert ^{40}Ca core. With the computer resources currently available to us, we can diagonalize these model states in the full $2s_{1/2}$, $1d_{5/2}$, $1d_{3/2}$, $1f_{7/2}$, $1f_{5/2}$, $2p_{3/2}$, and $2p_{1/2}$ configurational spaces (labeled *sdpf*) mentioned above but cannot do so for $A>43$; i.e., $(2s,1d)^{23}(1f,2p)^5$ is somewhat beyond our present capabilities—mainly disk storage space. Thus we are interested in a detailed comparison with experiment for various aspects of spectroscopy for $A=43$. This comparison should provide a test of the applicability of the spherical shell model to nuclei in the $A\sim 41-44$ region where shell-model calculations on the scale undertaken here have not been previously attempted.

The beta decay of ^{43}K has not been studied experimentally since 1970. Various technical advances such as larger Ge γ-ray detectors and more accurate γ-ray efficiency standards make it possible to obtain considerably more accurate beta matrix elements with not much effort. In particular, the nonunique first-forbidden branches to the first- and second-excited states of ^{43}Ca are weak and their determination involves the differences between two large values; namely, the γ-cascade intensities into and out of the two levels. Accordingly, a careful measurement of γ-ray intensities is needed in order to determine these two β^- branches as accurately as possible if the straightforward method of γ-ray intensity determinations is to be used.

In the next section (Sec. II) we describe the measurements on delayed γ rays following ^{43}K decay and compare the results to previous studies. Shell-model predictions of the ^{43}K(β^-) ^{43}Ca β^- matrix elements and of other observables are described in subsequent sections.

II. EXPERIMENTAL DETERMINATIONS FOR ^{43}K(β^-) ^{43}Ca

A. Source preparation and counting procedures

^{43}K, with $t_{1/2}=22.3(1)$ h (Ref. 10), was produced in the ^{44}Ca(t,α) ^{43}K reaction using tritons of $E_t=3.2$ MeV from the Brookhaven National Laboratory Van de Graaff accelerator. The target consisted of a 6-mm-diam pellet made from 92 mg of $CaCO_3$ enriched to 98.6% in ^{44}Ca. This was held on a support by means of a clamped 1-mg/cm^2-thick Ni foil. Activation consisted of bombarding the target for 8 h with a 200-nA triton beam.

In addition to ^{43}K other activities produced included ^{46}Sc ($t_{1/2}=83.3d$) from the ^{44}Ca(t,n) reaction, and ^{18}F ($t_{1/2}=110$ min) from the ^{16}O(t,n) ^{18}F reaction. The two γ rays of 889 and 1121 keV from ^{46}Sc were not so strong as to interfere with the ^{43}K measurements, but were in fact of sufficient strength to serve as energy standards in some of the work described below. However, the 511-keV annihilation radiation from the β^+ decay of ^{18}F was initially extremely strong. Thus measurements on the ^{43}K activity were delayed by 19 h after the end of the bombardment in order to allow the ^{18}F activity to decay.

Three series of measurements were carried out using a Ge(Li) detector. Relative γ-ray intensities were measured, first in two 3-h runs at a source-to-detector distance of 15.0 cm, and then in two 3-h runs at $d=8.2$ cm. Finally the ^{43}K was combined with a source of ^{192}Ir at distances of 4–8 cm for precision determinations of the ^{43}K γ-ray energies. Four such runs were made. After

completing the ^{43}K measurements, two different ^{152}Eu sources were used at the 8.2- and 15.0-cm distances for γ-ray efficiency calibrations. These spectra were taken with very good statistics so as to accurately evaluate not only the efficiency function but the γ-ray summing effects at the two distances.

B. β^- branching ratios

Detectable β^- branches from ^{43}K ($J^\pi=\frac{3}{2}^+$) can be expected to lead to all five of the lowest-lying ^{43}Ca levels.[10] The decay is predominantly (91%) to the 990-keV $\frac{3}{2}^+$ third-excited state. From magnetic spectrometer measurements it was determined that the branch to the $\frac{7}{2}^-$ ground state has the expected unique first-forbidden shape and a relative branching ratio (BR) of BR(g.s.)/BR(990 keV)=0.019 (Ref. 11) and 0.015 (Ref. 12). Uncertainties are not quoted. Based on the degree of agreement and our experience in similar analyses, we assign an uncertainty of 12% and assume 0.017(2) for this relative branch.

The beta branching to excited states is obtained from measurements of relative γ-ray intensities following ^{43}K decay. Four previous studies have been made using Ge spectroscopy.[13-16] The results of these studies have been reviewed by Waters.[16] His results are considerably more accurate than the previous ones and we need only consider them in any comparison to previous ^{43}K(β^-) ^{43}Ca γ-ray measurements.

The difficult β^- branch to obtain is that to the $\frac{5}{2}^-$ first-excited state at 373 keV. The difficulty is that the branch is weak and the three higher-lying levels fed in β^- decay all have large γ-decay branches to this state, thus, the net β^- intensity feeding this state is

$$I_\beta(1)=I_\gamma(1\rightarrow 0)-\sum_{i=2}^{4} I_\gamma(i\rightarrow 1)\ , \tag{1a}$$

where the states are labeled 0–4 starting with the ground state. To anticipate, one of our spectra gives

$$I_\beta(1)=41017-(2262+37\,389+920)=445 \text{ counts} \tag{1b}$$

and it is clear that a determination of this β^- branch depends on an accurate extraction of the relative γ-ray intensities.

Thus a critical part of the γ-intensity determinations is the calibration of the relative full-energy-loss efficiency, ϵ, as a function of γ-ray energy. For this we used a ^{152}Eu source placed at the same position as the ^{43}K source. Relative intensities of ^{152}Eu γ rays were most recently measured by Yoshizawa *et al.*,[17] who reviewed previous determinations. The results of Yoshizawa *et al.*[17] are the most accurate for the more intense γ transitions and we use them in our efficiency calibrations. The most critical γ intensities of Eq. (1) are the 373- and 617-keV γ rays. These energies are relatively close to the ^{152}Eu(β^+)^{152}Gd cascade 1123→344→0 which consists of 778- and 344-keV γ rays. To illustrate the accuracy possible, the intensity ratio for these two transitions from Ref. 17 has an accuracy of 0.59%. The degree of summing of γ cascades for both the ^{152}Eu and ^{43}K sources was assessed and accurately corrected for by determination of the sum peak at 1123 keV from 344+778 keV. This is possible because there is no known crossover from the ^{152}Gd 1123-keV level to the ground state. This sum peak was 0.38% and 0.19% of the 778-keV intensity for the measurements at 8.2 and 15.0 cm, respectively.

TABLE I. Relative intensities of γ rays observed following the β^- decay of ^{43}K.

E_γ (keV)	Relative intensity Present	Waters (Ref. 16)[a]
221	55.3(7)	47.0(25)
373	1000	1000
397	136.5(9)	131.0(24)
404	4.20(15)	1.25(9)
593	129.7(9)	126.4(40)
617	911.5(70)	923(15)
801	1.70(15)	1.69(12)
990	3.3(4)	3.8(7)
1022	22.6(3)	21.5(9)
1394	1.51(9)	1.17(14)

[a]The uncertainties assigned by Waters appear to be mainly statistical and do not adequately cover systematic errors in the relative efficiency and in peak area extractions. From the description of the experimental method it would appear that an additional systematic uncertainty of 2–5% should be added in quadrature.

The relative efficiency was parametrized by [18]

$$\ln(\epsilon_i)=\sum_{n=0}^{5} a_n[\ln(E_{\gamma i})]^n \tag{2}$$

and the a_n were determined by a least-squares fit to ~26 γ-ray intensities from 122 to 1408 keV for both the 8.2- and 15-cm spectra. The resulting efficiency curve for $E_\gamma>250$ keV had very closely the form $\epsilon_i=E_{\gamma i}^{-k}$ with $k\sim 0.9$.

Peak areas for the ^{152}Eu and ^{43}K spectra were extracted with the least-squares fitting routine SAMPO (Ref. 19). Three ^{43}K spectra were analyzed. The results were in good agreement and we list the overall results for the γ-ray intensities in Table I. The β^- branching ratios derived from Table I are listed in Table II. The results of Waters are also included in Tables I and II. The results of Table I also yield γ-ray branching ratios. These were extracted and are compared to previous results in Table III.

TABLE II. ^{43}K(β^-) ^{43}Ca β^- branching ratios to the five energetically accessible ^{43}Ca levels.

E_x (keV)	Branching ratio (%) Present	Waters (Ref. 16)[a]
0	1.54(18)[b]	1.6(2)[b]
373	0.9(6)	0.8(14)
593	4.06(13)	3.6(4)
990	90.9(6)	91.8(2)
1394	2.60(4)	2.2(1)

[a]See footnote a of Table I.

[b]From the results of Refs. 11 and 12 (see text).

TABLE III. Least-squares adjusted transition and level energies and gamma-ray branching ratios for the first four excited states of ^{43}Ca.

E_i (keV)	E_f (keV)	E_γ (keV)	Branching ratio (%) Present	^{40}Ar($\alpha,n\gamma$)[a]
372.762(7)	0			
593.394(6)	0	593.390(6)	70.2(3)	70.9(5)
	373	220.632(5)	29.8(3)	29.1(5)
990.257(8)	0	990.245(8)	0.31(4)	0.28(3)[b]
	373	617.490(6)	86.74(12)	87.1(3)
	593	396.861(6)	12.95(11)	12.6(3)
1394.473(14)	0	1394.448(14)	5.0(3)	5.0(4)
	373	1021.698(13)	75.3(7)	77.6(4)
	593	801.070(13)	5.6(5)	5.7(4)
	990	404.214(13)	14.1(5)	11.7(4)

[a]Reference 20.
[b]Reference 21.

C. Precision energy measurements

Energy measurements of the delayed γ rays following ^{43}K decay were made by the mixed-source technique[22] using standard procedures as in previous determinations at this laboratory.[23,24] The energy of the 1022-keV line was determined relative to the ^{46}Sc γ ray of 1120.545(4) keV (Ref. 25) in the three spectra recorded for relative intensity measurements. The other determinations summarized in Table IV were made from four spectra of mixed ^{192}Ir and ^{43}K. The ^{192}Ir reference energies of Table IV are from Ref. 25. A least-squares adjustment (LSA) of the ^{43}Ca γ-ray energies results in the γ-ray and level energies of Table III.[26] These are our suggested "best" energies. The results described here are summarized in the ^{43}K decay scheme of Fig. 1.

D. Comparison to previous results

The results of Waters[16] on relative γ intensities and β^- branching ratios are included in Tables I and II in order to represent previous measurements. It is seen that the present results are considerably more accurate. Allowing

TABLE IV. Summary of precision energy measurements for γ-ray transitions in ^{43}Ca. All reference energies are from Ref. 25.

E_γ (keV)	^{192}Ir reference (keV)	Δ (Ref.$-E_\gamma$) (keV)
220.633(5)	205.79550(7)	−14.837(5)
372.760(10)	316.50800(15)	−56.252(10)
396.867(10)	468.0715(2)	71.205(10)
404.201(15)	468.0715(2)	63.871(15)
593.390(7)	588.5851(5)	−4.805(7)
617.486(6)	612.466(2)	−5.020(6)
1021.720(20)	1120.545(4)[a]	99.825(20)

[a]^{46}Sc.

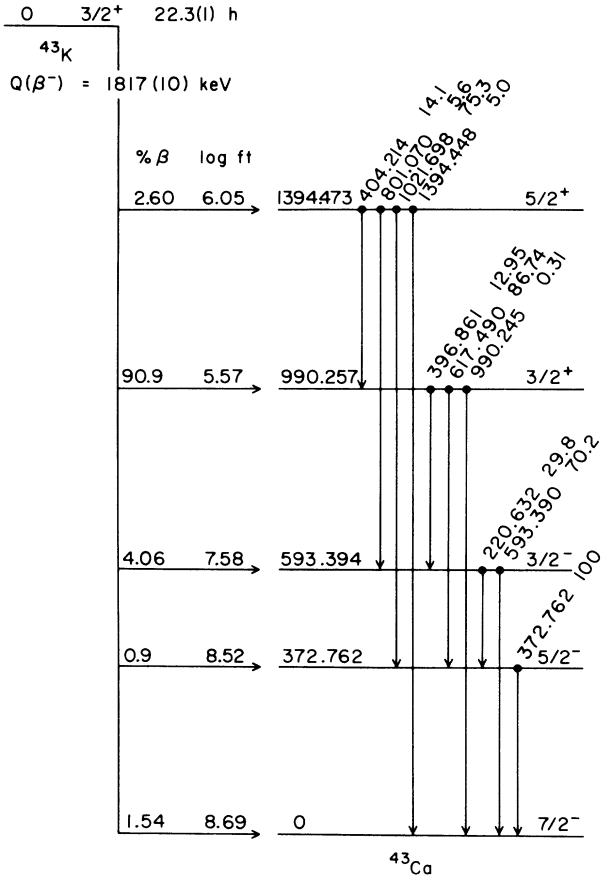

FIG. 1. Decay scheme for ^{43}K. The results are taken from those listed in the tables (present results) and discussed in the text, or from Ref. 10. All energies are in keV. The numbers to the left are the β^- branching ratios (in %) and logf_0t values. The γ-ray transitions are labeled by their energies from Table III and level branching ratios (in %).

for the fact that Water's results do not include systematic uncertainties (see footnote a of Table I), the two sets of intensities (Table I) and the β^- branching ratios derived from them (Table II) are in fair agreement. The two disagreements are in the intensities of the 404- and 1394-keV transitions which deexcite the 1394-keV level. In particular, we observe 3.4 times more 404-keV intensity than Waters. We can see no experimental difficulty with the 404-keV peak in our measurements. Its intensity relative to the 397-keV peak was the same to within ±15% over two half-lives and, as shown in Fig. 2, it is a clean, well-defined peak.

There are no previous γ-ray energy determinations of comparable accuracy to ours. Previous results (Ref. 10) agree within their uncertainties with ours.

We present the γ-ray branching ratios derived from the intensities of Table I in Table III where they are compared to results of Behbehani *et al.*[20] which were obtained via the ^{40}Ar($\alpha,n\gamma$) ^{43}Ca reaction. The two sets of results are in fair agreement except for the 404-keV 1394→990 transition which, once again, we find to be more intense than previously observed. We note the good agreement for the very weak 990→0 branching ratio with the careful determination of Holland and Lynch.[21] Our determination includes a large correction for summing; hence the relatively large uncertainty.

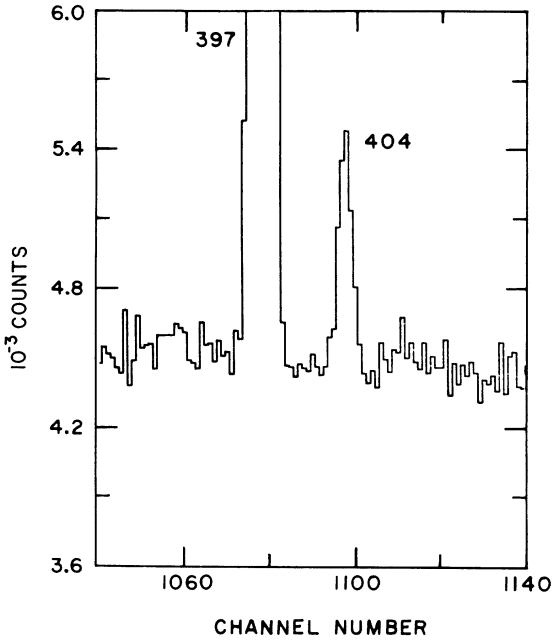

FIG. 2. Partial spectrum illustrating the 404-keV 1394→990 transition in ^{43}Ca following the decay of ^{43}K. The peaks are labeled by their energies in keV. The 397-keV peak rises to a maximum of 35×10^3 counts per channel.

E. Extraction of matrix elements

Comparison to theory for the allowed β^- transitions is best made via Gamow-Teller (GT) beta transition strength $B_{GT}\equiv B_0$. For the unique first-forbidden decay an analogous transition strength, B_1, can be defined, thus

$$B_n = 6166\left\{\frac{[(2n+1)!!]^2}{(2n+1)}\right\}\lambda_{Ce}^{2n}(f_n t)^{-1} . \tag{3a}$$

Equation (3a) gives

$$B_0 = 6166/f_0 t, \quad 10^{-6}B_1 = 2758/f_1 t \text{ fm}^2 , \tag{3b}$$

where f_0 and f_1 are Fermi functions calculated with shape factors of unity and $(q^2+\lambda_2 p^2)$, respectively, where λ_2 is a Coulomb function, differing negligibly from unity in the present application, and q and p are the neutrino and electron momentum, respectively. The Fermi integrals necessary for the evaluation of Eq. (3) were determined as described previously.[8] For the two nonunique decays comparison to the various matrix elements contributing to the decay rate cannot be separated and comparison to experiment is conventionally made via the f value defined by

$$ft = 6166 \text{ sec} , \tag{4a}$$

where t is the partial half-life of the transition and

$$f = \int_1^{W_0} C(W)F(Z,W)(W^2-1)^{1/2}W(W_0-W)^2 dW . \tag{4b}$$

The integrated Fermi function f is related to the decay rate Λ by

$$\Lambda(\text{sec}^{-1}) = 1/\tau = \ln 2/t = f/8896 . \tag{4c}$$

In Eq. (4b) $C(W)$ is the shape factor which contains all the information on the nuclear matrix elements.[8] The B_n and f values defined by Eqs. (3) and (4) are listed in Table V along with the associated values of $\log_{10} f_n t$.

TABLE V. Beta transition strengths (B_n), $\log_{10} f_n t$ values, and f values for the five β^- decays of ^{43}K [Eqs. (3) and (4)]. Uncertainties are enclosed in parentheses and powers of 10 in brackets. $\log_{10} f_0 t$ is listed for the nonunique decays.

^{43}Ca level				B_n or f	
J^π	(keV)	n	$\log_{10} f_n t$	Experiment	WBMB
$\frac{7}{2}^-$	0	1	9.71(5)	$B_1 = 5.4(6)[-4]$	3.9[−4]
$\frac{5}{2}^-$	372.762	nonunique	8.52(29)	$f = 7(5)[-4]$	2.5[−4]
$\frac{3}{2}^-$	593.394	nonunique	7.575(20)	$f = 3.12(10)[-3]$	0.81[−3]
$\frac{3}{2}^+$	990.257	0	5.567(20)	$B_0 = 1.67(8)[-2]$	4.4[−2]
$\frac{5}{2}^+$	1394.473	0	6.049(38)	$B_0 = 5.5(5)[-3]$	4.8[−3]

Also included in Table V are our shell-model predictions for the five transition strengths or f values. The calculation of these values is described in Sec. III A 1. The results will be discussed in the context of all the shell-model predictions in Sec. IV.

III. SHELL-MODEL CALCULATIONS

A. The interaction and its application

The spherical shell-model calculations discussed here use the WBMB interaction[8] which consists of the $(2s,1d)$ interaction of Wildenthal,[27] the $(1f,2p)$ interaction of McGrory,[28] and a modified[8] Millener-Kurath interaction[29] for the cross-shell interaction between the $(2s,1d)$ and $(1f,2p)$ shells. Nuclear structure results obtained with this interaction have been described fully elsewhere.[7-9] Calculations were done with the computer code OXBASH (Ref. 30). OXBASH works in the m scheme but utilizes projected basis vectors which have good J and T. The calculations in the full $(2s,1d)^{23}(1f,2p)^4$ model space involve quite large matrices: the J dimension for $J^\pi=\frac{7}{2}^+$, $T=\frac{3}{2}$ is 4517. Thus the calculations were quite time consuming and a clear physical picture of the wave functions is not always possible.

1. *Effective beta and electromagnetic decay operators*

The experimentally deduced observables for allowed and first-forbidden beta decay were described in Sec. II E. In calculating these observables we use effective operators derived in order to approximate the effects of nonnucleonic degrees of freedom and inadequacies of our shell-model space. The operators used in first-forbidden beta decay were described at length in a recent report[7,8] on first-forbidden beta decay near $A=40$ which contains a description of the calculation of the three $^{43}\mathrm{K}(\beta^-)\,^{43}\mathrm{Ca}$ branches of concern here.

For the GT operator—and the similar $M1$ electromagnetic operator—Brown and Wildenthal[31] extracted effective operators for the sd shell from a least-squares fit to GT and $M1$ matrix elements. We use their results for the sd shell. Our choice of effective operators for the fp shell is based on the good general agreement between the sd-shell operators of Brown and Wildenthal[31] and results obtained from general considerations.[32-34] Thus our effective fp operators are the fundamental results of Towner[34] modified to reproduce exactly the experimental $^{41}\mathrm{Sc}(\beta^+)\,^{41}\mathrm{Ca}$ GT matrix element and the ^{41}Ca and ^{41}Sc magnetic moments.

The corrections to isospin-allowed $M1$ decays and Gamow-Teller transitions are dominated by the isovector spin component. Thus we adjust this component in order to reproduce the experimental $A=41$ isovector magnetic moment and the Gamow-Teller decay of ^{41}Sc to ^{41}Ca. The isoscalar $A=41$ magnetic moment is reproduced by adjusting the isoscalar g_l value for the $f_{7/2}$ orbit. We do this because the Brown-Wildenthal[31] and Towner[34] corrections for the d orbits are in close agreement for g_s and poor agreement for g_l and we are inclined to expect the same behavior for the f orbits. This procedure will give corrections for the $f_{7/2}$ orbit. We assume the resulting corrections apply for the other fp matrix elements as well.

The $E2$ effective charges derived by Brown and Wildenthal from consideration of $E2$ decays and quadrupole moments in the sd shell are either $e_p,e_n=1.35,0.35$ if the incremental increases are constrained to be equal or $e_p,e_n=1.29,0.49$ if they are allowed to differ.[35] The agreement with experiment for sd-shell nuclei is not too much different in the two cases. We use identical effective charges in the sd and fp shells and adopt the asymmetric charges since results for $E2$ decays in ^{40}K give better agreement in this case than for the $e_n=0.35$ set.

2. *Two-nucleon transfer*

In general, the separation between nuclear structure and nuclear reaction dependencies cannot be made for two-nucleon stripping as it can for single-nucleon stripping. However, under some circumstances a quantitative understanding of the relative cross sections of two-nucleon reactions for a given angular momentum transfer L can be had from a consideration of spectroscopic amplitudes derived under the assumption that just such a separation can be made. Following Anyas-Weiss *et al.*,[36] we assume transfer of a structureless cluster and describe the nuclear states by a shell model with harmonic oscillator (HO) wave functions, then the wave function of the transferred nucleons is projected onto an internal state $0s$, which has no oscillator quanta, times a center-of-mass (c.m.) function containing all the quanta, $Q=2N-2+L$, and orbital angular momentum L of the transferred cluster, where N is the principal quantum number. In this way we pick out the component of the radial wave function which is largest at the nuclear surface and thus responsible for the bulk of the direct transfer of the cluster. There are reasons why this is a sensible procedure for both the (t,p) and (α,d) reactions being considered here. First, for the (t,p) reaction we make the usual assumption of transfer of an $S_k,T_k=0,1$ cluster and so, with this assumption, the projection is exact. For the (α,d) reaction, it is well known[37-39] that geometrical and kinematical factors strongly favor just this component of the wave function.

If now we restrict ourselves to the transfer of clusters with the same $(Q,0)$ structure, the radial wave functions of all jj components of the transferred cluster will be identical (using HO wave functions) and we can separate the nuclear structure and nuclear reaction dependencies for both the (t,p) and (α,d) reactions.

The shell-model calculations provide us with jj-coupling parentage coefficients $A(j_1,j_2)$ for the two-nucleon cluster. The two-nucleon spectroscopic amplitude is obtained by a transformation from the internal coordinates of the shell-model wave functions to a relative coordinate system for the cluster and the $A-2$ parent. A transformation from jj to LS coupling must also be made. Thus the basic spectroscopic amplitude is defined as

$$\theta(LJS_kT_k)=\left[\frac{A}{A-2}\right]^{Q/2}\times\sum_{j_1\geq j_2}\left[\frac{2}{1+\delta_{j_1j_2}}\right]^{1/2}\times\begin{Bmatrix} l_1 & \frac{1}{2} & j_1 \\ l_2 & \frac{1}{2} & j_2 \\ L & S & J \end{Bmatrix} A(j_1j_2)\mathrm{TM}\ , \quad (5)$$

where TM is the Talmi-Moshinsky bracket[40] for the change of coordinates. In general, for each final state, possible values of J for the cluster are

$$|L-S_k|\leq J\leq|L+S_k| \quad (6)$$

and the total cross section for specific L is

$$\sigma_L(S_kJ_f)=\Xi_L(S_k)\sigma_f(\mathrm{DWBA})\ , \quad (7)$$

where

$$\Xi_L(S_k)=(2J_f+1)\sum_J[\theta(LJS_kT_k)]^2 \quad (8)$$

contains all the dependence on the structure of the final state while σ_f(DWBA) accounts for all other factors including the Q dependence of the reaction.

B. ^{43}K

1. Previous calculations

Recent calculations for the even-parity states of ^{43}K have been made by Johnstone[41] and Chuu *et al.*[42] Both calculations used an

$$(s_{1/2}d_{3/2})^{-1}(f_{7/2},p_{3/2})^4$$

model space and calculated energy spectra and ^{44}Ca(d,^{3}He) ^{43}K spectroscopic factors. Since the $d_{5/2}$, $p_{1/2}$, and $f_{5/2}$ orbits should be of minor importance for these observables, we expect good agreement with our results performed in the

$$(d_{5/2}s_{1/2}d_{3/2})^{-1}(f_{7/2},p_{3/2},p_{1/2},f_{5/2})^4$$

model space. We are also interested in predictions for the ^{41}K(t,p) ^{43}K two-neutron transfer strengths and electromagnetic decay strengths.

2. Energy spectrum

Mordechai, Fortune, and Clement[43] (MFC) presented an interesting view of the positive parity states of ^{43}K interpreted as weak coupling of a $\pi d_{3/2}$ hole to states of ^{44}Ca. They developed this model and compared it to L values and relative cross sections they observed in the ^{41}K(t,p) ^{43}K reaction. Our approach to ^{43}K is influenced by theirs. Energy levels for ^{43}K and ^{44}Ca are shown in Fig. 3. For both nuclei the energy level spectrum predicted by the WBMB is compared to experiment. The predicted ^{43}K spectrum is offset so as to minimize the root-mean-square difference in excitation energies for the levels connected by solid lines to the experimental levels with which they are identified. The experimental spectrum for ^{44}Ca is from Endt and van der Leun,[10] that for ^{43}K is from ^{41}K(t,p) ^{43}K (Ref. 43), ^{43}Ar(β^-) ^{43}K (Ref. 44), and ^{40}Ar(α,$p\gamma$) ^{43}K (Ref. 45) studies, as well as from Endt and van der Leun.[10]

The ^{41}K(t,p) ^{43}K L-value assignments of MFC are shown in Fig. 3. MFC interpreted the two levels with $L=0$ as weak coupling of $\pi d_{3/2}^{-1}$ to the two lowest 0^+ levels of ^{44}Ca, and the four levels with $L=2$ and $L=4$ as the quartets formed in weak coupling of $\pi d_{3/2}^{-1}$ to the 2_1^+ and 4_1^+ levels of ^{44}Ca. The ^{44}Ca 1884-keV state is an intruder—supposedly from $n\hbar\omega$ ($n=2,4,\ldots$) excitations of $(2s,1d)^{24}(1f,2p)^4$—and thus is not predicted. In the weak-coupling model, we expect an extra $\frac{3}{2}^+$ state at $\sim$2 MeV in ^{43}K with no counterpart in the predicted spectrum. There are actually three possible $\frac{3}{2}^+$ excited

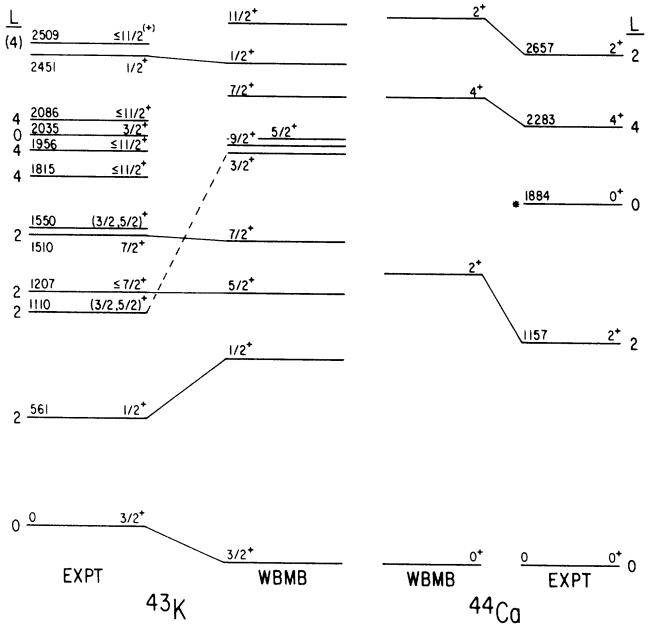

FIG. 3. The low-lying levels of ^{43}K and ^{44}Ca. For ^{44}Ca the experimental data are from Ref. 10 and known and predicted levels below 3-MeV excitation are shown. The L values on the right-hand side are those demanded for the ^{42}Ca(t,p) ^{44}Ca reaction by the indicated J^π assignments. For ^{43}K the experimental data are from Refs. 10 and 43–45 and the L values on the left-hand side are the ^{41}K(t,p) ^{43}K assignments of Mordechai *et al.* (Ref. 43). All even-parity states up to 1.6 MeV are shown; above 1.6 MeV only the $\frac{1}{2}^+$ state at 2451 keV and the states assigned $L=0$ or 4 by Mordechai *et al.* (Ref. 43) are shown. Other possible even-parity states are at 1866 and 2190 keV (Ref. 44) and 2040 keV (Ref. 45). The WBMB spectrum is shifted upwards in energy so as to minimize the rms deviation with experiment for the five levels connected to their experimental counterparts by solid lines. The association indicated by the dashed line is considered less certain than the others. With the shift shown (196 keV) the predicted binding energy is −369 203 keV, which is 405 keV more bound than experiment, and the rms deviation of the five excitation energies is 163 keV.

states below 2.6 MeV, at 1110, 1550, and 2035 keV. In contrast, the predicted $3/2_k^+$ levels for $k=1$, 2, and 3 are at the considerably higher excitation energies of 2133, 2954, and 3239 keV. It appears likely that two of the three experimental levels in question are intruders, one associated with $\pi d_{3/2}^{-1}\otimes{}^{44}$Ca (1884 keV) and one with the $\frac{3}{2}^+$ or $\frac{5}{2}^+$ level which arises from $\pi d_{3/2}^{-1}$ coupled to the first 2^+ intruder state. Following MFC we tentatively identify the 1110-keV level as arising primarily from $3/2_2^+$ of $(2s,1d)^{23}(1f,2p)^4$ and attribute its low excitation energy as due to the influence of the higher-lying $\frac{3}{2}^+$ intruders.

3. *Spectroscopic strength in proton pickup from ^{44}Ca*

The WBMB predictions for the spectroscopic factor S_p^- for the proton pickup of ^{44}Ca to $\frac{1}{2}^+$, $\frac{3}{2}^+$, and $\frac{5}{2}^+$ states of ^{43}K are given in Table VI for the first five states ($k=1-5$) of each spin. The definition of S_p^- is such that

$$\sum_{\substack{\text{fixed } J_f \\ \text{all } k}} S_p^-(J_f,k)=\frac{2T_f+1}{2T_f}(2J_f+1)\ . \tag{9}$$

It is seen that almost all of the pickup strength is predicted to reside in the first few states for $J^\pi=\frac{1}{2}^+$ and $\frac{3}{2}^+$. For $J^\pi=\frac{5}{2}^+$ the strength is predicted to lie above 6-MeV excitation. Results for the low-lying states are compared to experiment and to previous predictions in Table VII. The agreement is quite good. Doll *et al.*,[46] whose experimental results are shown in Table VII, found further $l=2$ spectroscopic strength in the energy region between 2.5 and 6.0 MeV. The summed strength for the 13 states in this region is $\sum S_p^-(l=2)=3.1$. The WBMB predicts a value of 1.2 for this sum. The disagreement suggests a redistribution of the spectroscopic strength due to $n\hbar\omega$ ($n=2,4,\ldots$) admixtures in the ^{44}Ca ground state and in the ^{43}K levels. A similar conclusion was reached by Doll *et al.*,[46] who discuss the distribution of $l=2$ strength from a different point of view.

4. *^{41}K(t,p) ^{43}K*

We follow MFC and neglect the kinematic differences in our comparison of the predicted (t,p) cross sections to experiment, i.e., the σ_f(DWBA) of Eq. (7) are assumed constant for given L. In Table VIII we list $1000\Xi_L$ where Ξ_L is as defined in Eq. (8). Our prediction is for the $L=0$ strength to be concentrated in $3/2_1^+$ as was observed experimentally. MFC do not give any information on the possible $L=0$ strength in the 1110- and 1550-keV levels. This information would be of interest. They report an $L=0$ cross section for the 2035-keV level which is 17% of that for the ground state.

Comparison of the relative cross sections for the ^{43}K $L=2$ levels of Fig. 3 is made in Table IX. The agreement is very good. Note the worst agreement is for the $3/2_2^+$ state, as we would expect from the presence of nearby intruder(s).

The J^π values for the $L=4$ quartet of Fig. 3 are all uncertain and their identification quite difficult. In Table X we compare the WBMB results to the experimental relative cross sections using the identification of the $L=4$ levels proposed by MFC. The WBMB predictions are in severe disagreement with experiment for the indicated choice of spin assignments. One reason for the disagreement is that MFC assume these four states exhaust the $L=4$ strength and, as is clear from Table VIII, the WBMB prediction is that this is far from the truth. For example, the $11/2_1^+$ model state is predicted to have its largest ^{44}Ca parentage in the 6_1^+ state rather than in 4_1^+ and the $L=4$ strength is fragmented over the $k=2-4$

TABLE VI. WBMB predictions for the spectroscopic factor S_p^- for the proton pickup of ^{44}Ca to ^{43}K.

k	$J^\pi;l_p=$ $\frac{1}{2}^+;0$	$\frac{3}{2}^+;2$	$\frac{5}{2}^+;2$
1	1.04	3.68	0.06
2	0.48	0.44	0.12
3	0.25	0.14	0.00
4	0.34	0.04	0.06
5	0.12	0.12	0.01
$\sum$	2.23	4.42	0.25
$\frac{5}{6}\sum/(2J+1)$	93%	92%	3%

TABLE VII. Comparison of the S_p^- of Table VI to experimental results for the low-lying states of ^{43}K and to previous predictions.

E_x (keV)	Model state	l_p	S_p^- Expt.[a]	WBMB	Ref. 41	Ref. 42
0	$3/2_1^+$	2	3.8	3.68	3.30	4.05
561	$1/2_1^+$	0	1.4	1.04	1.05	1.40
1110	$3/2_2^+$	2	0.6	0.44	0.29	
1207	$5/2_1^+$	(2)	(0.1)[b]	0.06		
1550	$(\frac{3}{2},\frac{5}{2})^+$	2	0.3	c		
2451	$1/2_2^+$	0	0.4	0.48	0.5	0.44

[a]Reference 46.

[b]Reference 47.

[c]Because of the relatively large value of S_p^-, this state is most likely $\frac{3}{2}^+$ (see Table VI); if so, it is most probably an intruder.

TABLE VIII. WBMB predictions for spectroscopic factors for the ^{41}K(t,p) ^{43}K reaction. k orders the levels by increasing energy. The quantity listed is $1000\Xi_L$ where Ξ_L is the spectroscopic strength of Eq. (8).

		$L=0$		
k	$J_f^\pi=\frac{3}{2}^+$			
1	368.2			
2	34.7			
3	53.2			
4	54.3			
5	13.8			
		$L=2$		
k	$J^\pi=\frac{1}{2}^+$	$\frac{3}{2}^+$	$\frac{5}{2}^+$	$\frac{7}{2}^+$
1	45.1	37.5	494.0	360.4
2	72.5	169.5	22.9	29.1
3	111.7	27.1	2.5	322.5
4	53.1	212.6	156.7	1.3
5	43.4	0.4	22.8	256.5
		$L=4$		
k	$J^\pi=\frac{3}{2}^+$	$\frac{7}{2}^+$	$\frac{9}{2}^+$	$\frac{11}{2}^+$
1	4.1	14.6	378.5	5.7
2	54.2	238.6	54.7	271.8
3	75.1	21.7	120.7	297.1
4	147.1	67.7	35.0	509.4
5	15.4	82.5	496.0	1.7

states. Better agreement with the predicted relative cross sections would result if the 2086- and 2509-keV levels were associated with $7/2_2^+$ and $9/2_1^+$, respectively, with the $k \geq 2$ $11/2_k^+$ states above the region of study. Obviously, more experimental work on the identification of spin and parities is needed before definite comparison to experiment can be made.

5. *Electromagnetic observables*

Predictions for electromagnetic observables for the lowest four even-parity states of ^{43}K are compared to experiment in Table XI. Two sets of predictions are given in the table; that labeled (b) uses the effective operators described in Sec. II B 1 while the predictions labeled (a) use the $M1$ operator appropriate to free nucleons and $E2$ effective charges of $e_p, e_n = 1.35, 0.35$. The "free" results are given so that the sensitivity to the choice of operators can be judged by comparison of the two predictions.

TABLE IX. Relative cross sections for the four ^{43}K $L=2$ levels of Fig. 3. The cross sections are normalized to a sum of 20.

E_x (keV)	Model state	Relative cross section Expt.	WBMB
561	$1/2_1^+$	0.9	0.8
1110	$3/2_2^+$	1.5	3.1
1207	$5/2_1^+$	10.0	9.3
1510	$7/2_1^+$	7.6	6.8
		20.0	20.0

TABLE X. Relative cross sections for the ^{43}K $L=4$ levels of Fig. 3. The cross sections are normalized to a sum of 36.

E_x (keV)	Model state	Relative cross section Expt.	WBMB
1815	$7/2_2^+$	4.3	12.7
1956	$9/2_1^+$	4.3	20.1
2086	$5/2_2^+$	11.3	2.9
2509	$11/2_1^+$	16.1	0.3
		36.0	36.0

The magnetic moment of the ^{43}K ground state is small due to cancellation between the spin and orbital contributions. It is interesting that the sign is different for the two predictions, indicating a strong sensitivity to the effective operators. Unfortunately the sign is not known experimentally.

The experimental information on the γ decays of the four listed excited states is rather scant; the predictions are in fair agreement with what information there is.

6. *Summary*

The WBMB gives a rather good picture of the first five even-parity states of ^{43}K. Considerably more experimental work is necessary on higher-lying even-parity states before meaningful comparison to theory can be made.

The picture of ^{43}K which emerges from the WBMB calculations is considerably more complex than a $\pi d_{3/2}^{-1} \otimes {}^{44}$Ca model would suggest. The first sign of this in the results we have presented is the large $l=0$ S_p^- for the $1/2_1^+$ state; i.e., it is not a good $\pi d_{3/2}^{-1} \otimes {}^{44}\mathrm{Ca}(2_1^+)$ state. The second sign is the fragmentation of the two-nucleon stripping strength (Table VIII). A further sign is the predicted values of the $E2$ transitions connecting the $\frac{1}{2}^+ - \frac{7}{2}^+$ quartet associated with a weak coupling $\pi d_{3/2}^{-1} \otimes {}^{44}\mathrm{Ca}(2_1^+)$ picture to the $\frac{3}{2}^+$ g.s. taken as $\pi d_{3/2}^{-1} \otimes {}^{44}\mathrm{Ca}(0_1^+)$. In such a model these should all be equal to the ^{44}Ca $2^+ \rightarrow 0^+$ $E2$ rate which is 10.2(7) Weisskopf units (W.u.).[10] The WBMB predictions, shown in Table XII, are seen to be in quite poor agreement with a weak-coupling picture.

C. ^{43}Ca

1. *Previous calculations*

The odd-parity spectrum of ^{43}Ca has been calculated in the full $(fp)^3$ space by McGrory.[28] Since we use the McGrory interaction for the (fp) part of our interaction, our results will be identical to his.

For the even-parity states the only shell-model calculation in a model space larger than $d_{3/2}^{-1} f_{7/2}^4$ appears to be the results of Chuu *et al.*[42] which also include the calculations for ^{43}K. Only energy spectra and ^{44}Ca(d,t) ^{43}Ca pickup factors are calculated.

We should also mention the very informative discussion of the even-parity states of ^{43}Ca by Behbehani *et al.*[20] Although no calculation is made, the local systematics are quite nicely elucidated.

TABLE XI. Comparison of experimental and predicted γ decays for the low-lying even-parity states of ^{43}K. The $B(L)$ are in Weisskopf units (W.u.), the $\mu(M1)$ are in nm, and the $Q(E2)$ are in e b. The phase convention is that of Rose and Brink (Ref. 48). Powers of 10 are given in square brackets and uncertainties in parentheses. The experimental information is from Refs. 10 and 43–45. The $E2$ observables in the columns labeled (a) and (b) are calculated with $e_p,e_n=1.35,0.35$ and 1.29,0.49, respectively. The $M1$ observables in these two columns are calculated with the "free nucleon" operator and the effective operator of Sec. III A 1, respectively.

Initial state		Final state		E_γ	τ	BR		Experimental	Predicted values	
E_i (keV)	J^π	E_f (keV)	J^π	(keV)	(psec)	(%)	Quantity	value	(a)	(b)
0	$\frac{3}{2}^+$	0	$\frac{3}{2}^+$				$\mu(M1)$	$\pm0.163(2)$	-0.099	$+0.116$
							$Q(E2)$	a	$+0.083$	$+0.092$
561	$\frac{1}{2}^+$	0	$\frac{3}{2}^+$	561	a	100	$B(M1)$	a	1.90[−2]	3.01[−3]
1110	$(\frac{3}{2})^+$	0	$\frac{3}{2}^+$	1110	a	70(3)	$B(M1)$	a	5.73[−3]	5.94[−3]
		561	$\frac{1}{2}^+$	549	a	30(3)	$B(M1)$	a	1.18[−2]	2.72[−2]
							$BR(\frac{1}{2}^+)$	30(3)%	31%	35%
1207	$(\frac{5}{2})^+$	0	$\frac{3}{2}^+$	1207	>7	100	$B(M1)$	<2.6[−3]	2.44[−3]	1.58[−4]
							$x(E2/M1)$	a	$+0.561$	-2.876
		561	$\frac{1}{2}^+$	646		<10	$B(E2)$	<11.6	0.38	0.36
1510	$\frac{7}{2}^+$	0	$\frac{3}{2}^+$	1510	8(2)	92(2)	$B(E2)$	1.3(3)	1.33	2.06
		1207	$\frac{5}{2}^+$	303		8(2)	$B(M1)$	1.1(4)[−2]	1.82[−2]	3.04[−2]
							$x(E2/M1)$	a	-0.058	-0.054

[a]Not measured.

2. *Energy spectra*

Predictions for the low-lying and yrast even-parity spectra of ^{43}Ca are compared to experiment in Figs. 4 and 5, respectively. The experimental results come almost entirely from the very comprehensive ^{40}Ar$(\alpha,n\gamma)$ ^{43}Ca study of Behbehani *et al.*[20] The fusion-evaporation study of Poletti *et al.*[49] assists in the location of Yrast states, and the ^{41}K(α,d) ^{43}Ca results of Nann *et al.*[39] assist in the identification of the high-spin states. Results other than those of Behbehani *et al.*[20] are reviewed by Endt and van der Leun.[10] We defer discussion of these spectra until Sec. IV.

3. *Spectroscopic strength in neutron pickup from ^{44}Ca*

The WBMB predictions for the spectroscopic factor S_n^- for the neutron pickup of ^{44}Ca to $\frac{1}{2}^+$, $\frac{3}{2}^+$, and $\frac{5}{2}^+$ states of ^{43}Ca are given in Table XIII for the first five states ($k=1-5$) of each spin. S_n^- is normalized so that

$$\sum_{\substack{\text{fixed } J_f \\ \text{all } k}} S_n^-(J_f,k)=(2J_f+1)\ . \tag{10}$$

Results for the low-lying states are compared to experiment and to previous predictions in Table XIV. Except for the $3/2_1^+$ state, our predictions are in poor agreement with experiment. This is especially true for the $1/2_1^+$ state for which the WBMB predicts far too little $l=0$ strength. Note that the calculation of Chuu *et al.*[42] does not have this deficiency. Another failure is one similar to that for ^{44}Ca$(d,^3$He$)$ ^{43}K (Table VII); namely, we predict less low-lying $l=2$ strength than is seen experimentally. In addition to the $l=2$ results of Table XIV, Doll *et al.*[46] observed $\sum_{3.1\text{ MeV}}^{6.0\text{ MeV}} S_n^-(l=2)=1.62$ for a total $\sum_{0\text{ MeV}}^{6.0\text{ MeV}} S_n^-(l=2)=5.2$ as opposed to a prediction of 3.1. As in the case of ^{43}K, the $l=2$ strength appears to be redistributed due to $n\hbar\omega$ ($n=2,4,\ldots$) admixtures in ^{44}Ca and ^{43}Ca levels.

TABLE XII. $E2$ transition strength for decay of the first four ^{43}K even-parity levels to the $\frac{3}{2}^+$ ground state calculated with $e_p,e_n=1.29,0.49$.

E_x (keV)	Model state	$B(E2)$ (W.u.)
561	$1/2_1^+$	5.24
1110	$3/2_2^+$	0.019
1207	$5/2_1^+$	2.58
1510	$7/2_1^+$	2.06

TABLE XIII. WBMB predictions for the spectroscopic factor S_n^- for the neutron pickup of ^{44}Ca to ^{43}Ca.

	$J^\pi;l_n=$		
k	$\frac{1}{2}^+;0$	$\frac{3}{2}^+;2$	$\frac{5}{2}^+;2$
1	0.14	2.54	1.6[−3]
2	0.02	0.06	8.1[−5]
3	0.32	0.10	9.6[−4]
4	0.17	0.00	3.7[−2]
5	0.06	0.03	3.0[−2]
$\sum$	0.71	2.73	0.07
$\sum/(2J+1)$	36%	68%	1.2%

4. $^{41}K(\alpha,d)\,^{43}Ca$

Nann *et al.*[39] studied the $^{41}K(\alpha,d)\,^{43}Ca$ reaction. As expected from the kinematical conditions, they observed large cross sections for $L=6$ and $L=4$ formation of even-parity states which they identified mainly as arising from $(sd)^{23}(fp)^4$. As discussed in Sec. III A 2, we have calculated the two-nucleon spectroscopic strengths Ξ_L of Eqs. (7) and (8) for $J^\pi=\frac{7}{2}^+-\frac{17}{2}^+$ states of ^{43}Ca. In comparing to the 10° experimental cross sections of Nann *et al.*,[39] we neglect any kinematical dependence, i.e., assume σ_f(DWBA) of Eq. (7) is dependent only on L. For the (α,d) reaction we assume $S_k,T_k=1,0$ so that for the

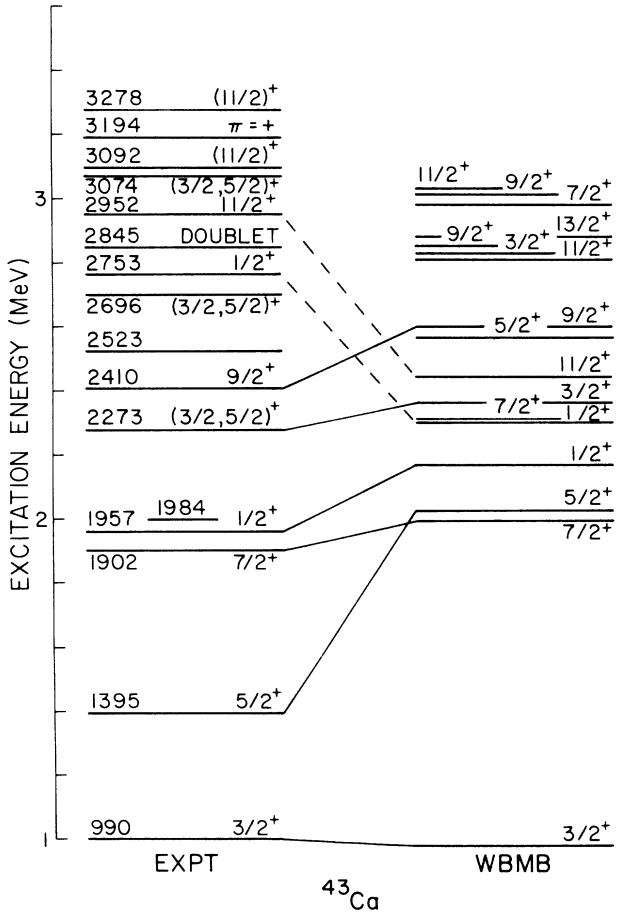

FIG. 4. The low-lying even-parity levels of ^{43}Ca. The experimental data are from Ref. 20. All known experimental even-parity levels below 3320 keV are shown; all predicted even-parity levels below 3750 keV are shown. The WBMB spectrum is shifted in energy so as to minimize the rms deviation with experiment for the excitation energies of nine levels: the six levels connected by solid lines to the experimental levels with which they are identified and also the $\frac{13}{2}^+$, $\frac{15}{2}^+$, and $\frac{17}{2}^+$ yrast levels (see Fig. 5). The identifications indicated by dashed lines are considered less definite. With the shift shown (-665 keV), the average binding energy is predicted to be $-368\,116$ keV, which is 724 keV less bound than experiment. The rms deviation for the excitation energies of the nine levels included in the comparison is 391 keV.

TABLE XIV. Comparison of the S_n^- of Table XIII to experimental results for the low-lying states and to previous predictions.

E_x (keV)	Model state	l_n	S_n^- Expt.[a]	S_n^- WBMB	S_n^- Ref. 42
990	$3/2_1^+$	2	2.7(4)	2.54	2.92
1395	$5/2_1^+$	2	0.16(13)	0.00	
1957	$1/2_1^+$	0	1.0(2)	0.14	1.18
2273	$3/2_2^+$	(2)	0.21(5)	0.06	
2696	$(\frac{3}{2},\frac{5}{2})^+$	2	0.23(7)	<0.1	
2845	$(\frac{3}{2},\frac{5}{2})^+$	2	0.28(5)	<0.1	
3074	$(\frac{3}{2},\frac{5}{2})^+$	2	0.52(10)	<0.1	
2753	$1/2_2^+$	0		0.02	

[a]Average value of those quoted in Table 43.11 of Ref. 10. The number in parentheses is the internal error of the measurement.

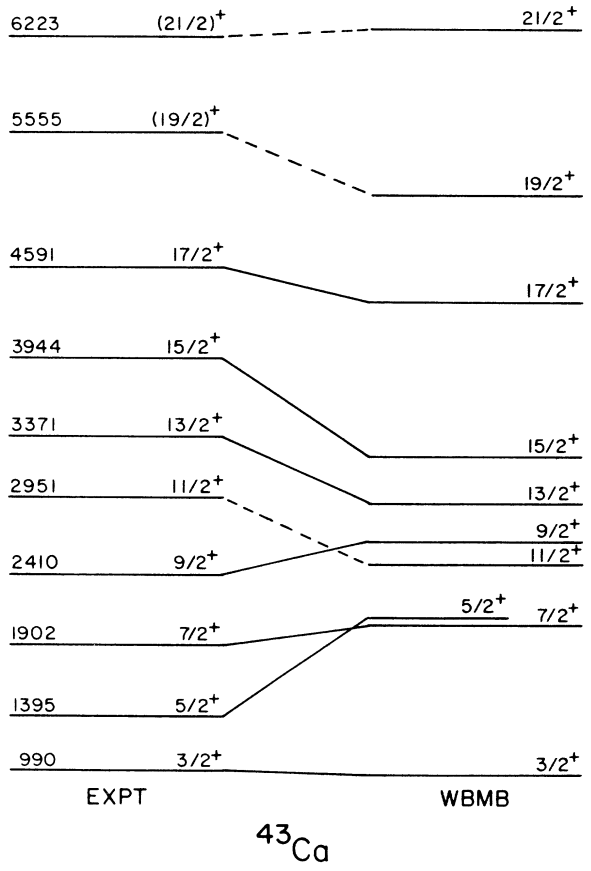

FIG. 5. The even-parity yrast states of ^{43}Ca. The experimental data are from Ref. 20. The WBMB predicted spectrum is positioned in energy as in Fig. 4. The identification between the predicted and experimental levels is indicated by solid or dashed (if less certain) lines.

transferred cluster three values of J ($=L, L\pm1$) are possible for each L. However, for both $L=4$ and $L=6$ our predictions are for essentially negligible contributions from $J=L, L-1$. Also, $L=4$ is dominated by $(p_{3/2}f_{7/2})^2_{J=5}$ and $L=6$ is dominated by $(f_{7/2})^2_{J=7}$; i.e., by the stretched configurations. These findings are just as predicted by Nann *et al.*[39] and by earlier studies.[37,38] The results are listed in Table XV. It is seen that the reaction is quite selective. First, note that $J^\pi=\frac{7}{2}^+$ and $\frac{9}{2}^+$ states are weakly formed for $L=6$. This reflects the $J=7$ dominance; i.e., strongly formed states are those with $\mathbf{J}_f=\frac{3}{2}+\mathbf{J}$. Second, note that for each J_f the cross sections vary widely. This is partly due to the coherent summing of the various j_1, j_2 contributions, but even for $J^\pi=\frac{17}{2}^+$ for which only $(f_{7/2})^2$ contributes, the Ξ values vary strongly, reflecting large differences in the parentage of the ^{43}Ca $\frac{17}{2}^+$ states for a $(f_{7/2})^2_{J=7}$ neutron-proton pair coupled to the ^{41}K ground state. Comparison of the predictions to experiment is made in Table XVI. In this comparison we rely on the identification of states made by Behbehani *et al.*,[20] whose excitation energies and spin-parity assignments are given in the first two columns. Our proposed model assignments are given in the third column, those in parentheses are conjectured on the basis of the present comparison. Because of the sensitivity of the Ξ_L values to the model wave functions and the approximations made in the derived relative cross sections, we expect only qualitative agreement with experiment. In actual fact the agreement is quite good with some notable successes. What is included in Table XVI are the eight states identified[39] as having $L=6$ cross sections within 10% of that for the strongest. One notable success is the fact that $13/2^+_1$ is predicted to be more weakly formed by both $L=4$ and $L=6$ than $13/2^+_2$ in agreement with experiment. Another is the similar situation for $15/2^+_1$ and $15/2^+_2$. Encouraged by this success we propose the identification of $13/2^+_4$ and $15/2^+_3$ with the 4137- and 4888-keV levels, respectively. These identifications follow from a perusal of the relative Ξ_L values and the predicted excitation energies of Table XV.

5. *Electromagnetic observables*

Predictions for electromagnetic observables for low-lying states of ^{43}Ca are compared to experiment in Table

TABLE XV. Relative values of Ξ_L for $L=4$ and 6 transfer to $J=\frac{7}{2}^+-\frac{17}{2}^+$ states of ^{43}Ca. The results are normalized to the experimental cross sections of Nann *et al.* (Ref. 39) for the $\frac{13}{2}^+$ state at 3500 keV for $L=4$ and the $\frac{17}{2}^+$ state at 4591 keV for $L=6$. For each $L=4$ entry and the last two columns for $L=6$, the predicted excitation energy is given in parentheses. The Q dependence of the cross section is neglected. Cross sections for $J<\frac{7}{2}$ are predicted to be negligible for both values of L. Entries which are considered too small to be of interest are given with the power of 10 in square brackets. k orders the states in energy.

					$L=4$			
k	$J_f=\frac{7}{2}$		$\frac{9}{2}$		$\frac{11}{2}$		$\frac{13}{2}$	
1	6.1[+0]	(2705)	11	(3309)	14	(3155)	4.5[+0]	(3566)
2	7.9[−1]	(3033)	33	(3562)	1.9[+0]	(3519)	130	(3933)
3	21	(3692)	6.3[+0]	(3725)	9.5[+0]	(3728)	7.3[+0]	(4332)
4	55	(3872)	1.6[−1]	(4100)	57	(4088)	2.3[−1]	(4591)
5	1.2[+0]	(4102)	67	(4453)	13	(4329)	7.4[−3]	(4954)
6	15	(4171)	30	(4532)	37	(4624)	86	(5192)
7	4.7[−1]	(4568)	53	(4822)	128	(4702)	240	(5419)
8	22	(4668)	3.9[+0]	(5099)	14	(4930)	1.4[−1]	(5905)
9	3.8[+0]	(4893)	28	(5140)	175	(5064)	52	(6222)
10	6.4[+0]	(5003)	17	(5156)	3.7[+0]	(5273)	160	(6404)

					$L=6$			
k	$J_f=\frac{7}{2}$	$\frac{9}{2}$	$\frac{11}{2}$	$\frac{13}{2}$	$\frac{15}{2}$		$\frac{17}{2}$	
1	1.7[−3]	1.0[−2]	43	23	52	(3911)	510	(5018)
2	1.1[−4]	4.3[−1]	1.2[+0]	120	233	(4333)	13	(5852)
3	1.7[−2]	1.2[−1]	1.1[+0]	30	60	(4986)	1.8[+0]	(6400)
4	2.0[−1]	3.2[+0]	94	78	8.3[−2]	(6102)	9	(6640)
5	1.6[−1]	9.4[−1]	1.1[+0]	19	1.5[−1]	(6148)	9.1[−1]	(6871)
6	1.1[−1]	4.3[−3]	5.3[−1]	46	4.1[+0]	(6494)	2.8[+0]	(7239)
7	1.1[−2]	7.1[−2]	9.1[+0]	7.6[+0]	4.5[+0]	(6512)	4.3[−1]	(7455)
8	3.3[−2]	5.2[−2]	3.0[+0]	2.4[+0]	6.5[−1]	(6819)	15	(7554)
9	1.9[−2]	2.6[−1]	4.5[+0]	2.2[+0]	1.6[+0]	(6998)	6.6[−1]	(7811)
10	1.7[−2]	8.5[−2]	6.7[+0]	1.4[+0]	1.3[+0]	(7037)	14	(8212)

TABLE XVI. Relative cross sections (μb/sr at 10°) in the ^{41}K(α,d) ^{43}Ca reaction. The experimental cross sections are due to Nann *et al.* (Ref. 39); the level identifications are from Ref. 20.

E_x (keV)	$2J^\pi$ Expt.	$2J_k^\pi$ WBMB	$\sigma(L=6)$ Expt.	$\sigma(L=6)$ WBMB	$\sigma(L=4)$ Expt.	$\sigma(L=4)$ WBMB
2951	11^+	11_1^+	76	43		14
3372	13^+	13_1^+	79	23		5
3500	13^+	13_2^+	110	120	130[a]	130[a]
3944	15^+	15_1^+	135	52		
4137	$(11,13)^+$	(13_4^+)	78	78		0.23
4186	15^+	15_2^+	220	233		
4591	17^+	17_1^+	510[a]	510[a]		
4888	$(11-17)^+$	(15_3^+)	105	60		

[a]The predicted cross sections for this value of L are normalized to this experimental cross section.

XVII, while the γ decays of the even-parity Yrast states of ^{43}Ca are considered in Table XVIII. The predictions are in very poor agreement with experiment, the only exception being the decays of the $J \geq \frac{15}{2}$ yrast states of Table XVIII. The most startling deficiency is for the $7/2_1^+ \rightarrow 3/2_1^+$ and $9/2_1^+ \rightarrow 5/2_1^+$ $E2$ rates which are experimentally very large. But the general agreement for the low-lying states of both parities is also very poor. These results essentially demand the participation of $n\hbar\omega$ ($n=2,4,\ldots$) excitations of the zeroth-order configuration for the even-parity states and probably for the odd-parity states as well. We will take up this subject in the next section.

TABLE XVII. Comparison of experimental and predicted γ decays for low-lying states of ^{43}Ca. The $B(L)$ are in Weisskopf units (W.u.), the $\mu(M1)$ are in nm, and the $Q(E2)$ are in e b. The phase convention is that of Rose and Brink (Ref. 48). Powers of 10 are given in square brackets and uncertainties in parentheses. The experimental information is from Refs. 10, 20, and 50. The $E2$ observables in the columns labeled (a) and (b) are calculated with $e_p,e_n=1.35,0.35$ and 1.29,0.49, respectively. The $M1$ observables in these two columns are calculated with the "free nucleon" operator and the effective operator of Sec. III A 1, respectively. Both columns use $e_p,e_n=1.5,0.5$ for $E3$ transitions.

Initial state E_i (keV)	J^π	Final state E_f (keV)	J^π	E_γ (keV)	τ (psec)	BR (%)	Quantity	Experimental value	Predicted values (a)	(b)
0	$\frac{7}{2}^-$	0	$\frac{7}{2}^-$				$(M1)$	−1.318	−1.683	−1.433
							$Q(E2)$	−4.9(5)	−1.43	−2.01
373	$\frac{5}{2}^-$	0	$\frac{7}{2}^-$	373	48(4)	100	$B(M1)$	1.3(1)[−2]	1.33[−3]	6.42[−4]
							$x(E2/M1)$	+0.192(11)	+0.190	+0.382
							$B(E2)$	3.5(5)	0.99	1.94
593	$\frac{3}{2}^-$	0	$\frac{7}{2}^-$	593	117(6)	70.2(3)	$B(E2)$	7.4(4)	4.33[−1]	8.49[−1]
		373	$\frac{5}{2}^-$	221		29.8(3)	$B(M1)$	7.5(6)[−3]	4.09[−4]	2.23[−4]
							$x(E2/M1)$	+0.10(5)	+0.189	+0.359
990	$\frac{3}{2}^+$	0	$\frac{7}{2}^-$	990	71(5)	0.28(3)	$B(M2)$	0.15(2)	0.83	0.83
							$B(E3)$	a	3.00	3.00
							$x(E3/M2)$	a,b	−0.028	−0.028
1395	$\frac{5}{2}^+$	990	$\frac{3}{2}^+$	404	3.4(11)	14.1(5)	$B(M1)$	1.5(5)[−2]	0.81[−2]	0.76[−2]
							$x(E2/M1)$	−0.32(5)	+0.095	+0.122
1957	$\frac{1}{2}^+$	990	$\frac{3}{2}^+$	967	1.55(46)	22(1)	$B(M1)$	<5.0(15)[−3]	1.54[−4]	1.16[−4]
							$x(E2/M1)$	a	+0.769	+1.036
2273	$(\frac{3}{2})^+$	990	$\frac{3}{2}^+$	1283	0.40(12)	84(3)	$B(M1)$	3.0(11)[−2]	2.51[−1]	2.17[−1]
							$x(E2/M1)$	+0.26(5)	+0.046	+0.056
							$B(E2)$	2.9(14)	0.93	1.19
		1395	$\frac{5}{2}^+$	877		16(3)	$B(M1)$	1.9(7)[−2]	0.369	0.353
							$x(E2/M1)$	−0.1(4)	+0.001	+0.001

[a]Not measured.

[b]Assumed zero in extracting the experimental value of $B(M1)$.

IV. DISCUSSION

A. Core excitations in mass 43

1. Orientation

The comparison of our shell-model predictions to experimental results for the $A=43$ nuclei ^{43}K and ^{43}Ca shows adequate agreement for the $T=\frac{5}{2}$ states and high-lying even-parity $T=\frac{3}{2}$ states but extremely poor agreement for the low-lying $T=\frac{3}{2}$ states. Among the points of disagreement are (1) the poor match in energy spectra (Fig. 4); particularly the $\frac{3}{2}^+$ states which we expect to be most influenced by core-excited intruders; (2) the disagreement in electromagnetic observables (Table XVII) such as the aforementioned $E2$ rates and the wrong sign of the $E2/M1$ mixing ratio of the $5/2_1^+ \rightarrow 3/2_1^+$ transition; and (3) the very poor agreement in the $l=0$ pickup strength to the $1/2_1^+$ level. These results suggest large core-excited admixtures in the low-lying $T=\frac{3}{2}$ states which are significantly greater than the ~ 15–$25\,\%$ normally found in light nuclei and presumably present in the higher-lying $T=\frac{3}{2}$ states and the $T=\frac{5}{2}$ states. Unfortunately, inclusion of even $2\hbar\omega$ com-

TABLE XVIII. Comparison of experimental and predicted γ decays for the even-parity yrast states of ^{43}Ca. The $B(L)$ are in Weisskopf units (W.u.), the $\mu(M1)$ are in nm, and the $Q(E2)$ are in e b. The phase convention is that of Rose and Brink (Ref. 48). Powers of 10 are given in square brackets and uncertainties in parentheses. The experimental information is from Refs. 10 and 20. The $E2$ observables in the columns labeled (a) and (b) are calculated with $e_p,e_n=1.35,0.35$ and 1.29,0.49, respectively. The $M1$ observables in these two columns are calculated with the "free nucleon" operator and the effective operator of Sec. III A 1, respectively.

Initial state		Final state		E_γ	τ	BR		Experimental	Predicted values	
E_i (keV)	J^π	E_f (keV)	J^π	(keV)	(psec)	(%)	Quantity	value	(a)	(b)
1902	$\frac{7}{2}^+$	990	$\frac{3}{2}^+$	911	0.72(19)	13(4)	$B(E2)$	26(11)	0.88	1.42
		1395	$\frac{5}{2}^+$	507		17(4)	$B(M1)$	5.7(23)[−2]	2.37[−1]	2.03[−1]
							$x(E2/M1)$	a,b	−0.005	−0.009
2410	$\frac{9}{2}^+$	1395	$\frac{5}{2}^+$	1015	1.6(6)	44(4)	$B(E2)$	23(9)	0.43	0.58
		1902	$\frac{7}{2}^+$	508		11(2)	$B(M1)$	1.7(6)[−2]	1.17[−2]	1.37[−2]
							$x(E2/M1)$	a,b	−0.010	−0.011
2951	$\frac{11}{2}^+$	1902	$\frac{7}{2}^+$	1050	6.8(17)	21(1)	$B(E2)$	2.2(6)	1.45	2.04
		2410	$\frac{9}{2}^+$	542		14(1)	$B(M1)$	4.1(10)[−3]	8.25[−2]	6.64[−2]
							$x(E2/M1)$	+0.04(2)	+0.008	+0.006
3371	$\frac{13}{2}^+$	2410	$\frac{9}{2}^+$	962	12(7)	41(1)	$B(E2)$	3.8(22)	1.30	1.57
		2951	$\frac{11}{2}^+$	420		21(1)	$B(M1)$	8(5)[−3]	4.18[−2]	5.31[−2]
							$x(E2/M1)$	a,b	−0.004	−0.005
3944	$\frac{15}{2}^+$	2951	$\frac{11}{2}^+$	992	1.1(3)	a	$B(E2)$	a	0.89	1.24
		3371	$\frac{13}{2}^+$	572		51(7)	$B(M1)$	7.9(24)[−2]	6.3[−2]	5.6[−2]
							$x(E2/M1)$	a,b	+0.002	+0.003
		3505	$\frac{13}{2}^+$	438		34(7)	$B(M1)$	1.2(4)[−1]	1.56[−1]	1.38[−1]
							$x(E2/M1)$	+0.00(2)	+0.006	+0.006
4591	$\frac{17}{2}^+$	3371	$\frac{13}{2}^+$	1220	0.300(75)	a	$B(E2)$	a	0.31	0.36
		3944	$\frac{15}{2}^+$	647		49(5)	$B(M1)$	0.19(5)	1.17[−1]	1.18[−1]
							$x(E2/M1)$	+0.00(2)	−0.008	−0.010
		4186	$\frac{15}{2}^+$	404		24(5)	$B(M1)$	3.8(12)[−1]	4.2[−1]	3.0[−1]
							$x(E2/M1)$	a,b	+0.025	+0.031
							$B(E2)$	a,b	4.71	5.21
5555	$(\frac{19}{2})^+$	3944	$\frac{15}{2}^+$	1611	1.95(55)	>40	$B(E2)$	>1.7(5)	0.76	1.24
		4591	$\frac{17}{2}^+$	964		<60	$B(M1)$	<1.1(3)[−2]	3.23[−3]	2.74[−3]
							$x(E2/M1)$	a,b	+0.022	+0.029
6223	$(\frac{21}{2})^+$	4591	$\frac{17}{2}^+$	1632	0.83(22)	a	$B(E2)$	a	2.69	3.57
		5555	$\frac{19}{2}^+$	668		100	$B(M1)$	1.28(33)[−1]	0.92[−1]	0.95[−1]
							$x(E2/M1)$	+0.02(3)	−0.005	−0.011

[a]Not measured.
[b]Assumed zero in extracting the experimental value of $B(M1)$.

ponents in our model space would greatly exceed our computational resources. But even if possible, a mixed $(0+2)\hbar\omega$ calculation would be of doubtful validity. The problem is that the low-lying $0\hbar\omega$ states have very large dominant off-diagonal interactions with $2\hbar\omega$ states of similar symmetry which lie $\sim$20 MeV above the lowest $2\hbar\omega$ states. This interaction greatly depresses the low-lying $0\hbar\omega$ states, thus greatly reducing their interaction with the low-lying $2\hbar\omega$ states. The problem arises because of truncation at $2\hbar\omega$, i.e., $4\hbar\omega$ states would also depress the low-lying $2\hbar\omega$ states, etc. (Refs. 51 and 52).

Highly truncated shell models can be constructed which do seem to work well enough in mixed $(0+2+\cdots)\hbar\omega$ model spaces to reproduce many features of low-lying levels. Examples are the $(p_{1/2}d_{5/2}s_{1/2})$ model of Reehal and Wildenthal[53] and the $(d_{3/2}f_{7/2})$ model of Hsieh *et al.*[54] which are applicable near $A=16$ and 40, respectively. These interactions avoid the $(0+2)\hbar\omega$ mixing quagmire (but, naturally, at great expense otherwise) because the $2\hbar\omega$ states of similar symmetry to the low-lying $0\hbar\omega$ states are omitted by the truncation. Calculations with the $(d_{3/2}f_{7/2})$ model give insight into the structure of the mass 43 levels in question.

Calculations with the Hsieh-Wildenthal interaction were carried out in a $d_{3/2}^{8-n}f_{7/2}^{3+n}$ model space with various restrictions on n. First we compare the $n=0$ and $n=1$ binding energies to those for $n=2$ and 3, respectively, i.e., the relative $0\hbar\omega$ and $2\hbar\omega$ binding energies for odd and even parity. This gives us an orientation toward the mixing of the zeroth-order configuration with core-excited states. For the ^{43}Ca odd-parity levels we find the core-excited states are predicted to commence with a $\frac{5}{2}^-$ state 0.54 MeV above the $\frac{3}{2}^-$ $n=0$ ground state. For the ^{43}Ca even-parity states the prediction is for a $\frac{3}{2}^+$ core-excited state 0.44 MeV above the $n=1$ $\frac{3}{2}^+$ state. These are quite small energy differences indeed, so we expect the model to give strong mixing of the $0\hbar\omega$ states with the core-excited states. By contrast the $n=3$ ^{43}K spectrum commences with a $\frac{3}{2}^+$ state 2.3 MeV above the $n=1$ $\frac{3}{2}^+$ state. If now we calculate mixed $n=0+2$ and $1+3$ spectra we find that indeed the low-spin, low-lying levels of ^{43}Ca are most strongly mixed, with up to $\sim$40% $2\hbar\omega$ admixtures (for $3/2_1^+$). As the spin and energy increase the mixing falls off to $\sim$15% of core excitation in the yrast states which is also the value found for ^{43}K. The reason for this seems to be simply that the low-lying, low-spin core-excited states are in close energy proximity with the corresponding $0\hbar\omega$ states and this proximity falls off rapidly with spin and energy. This gives us a qualitative understanding of the ^{43}Ca $E2$ rates of Table XVIII. The $\frac{7}{2}^+\rightarrow\frac{3}{2}^+$ and $\frac{9}{2}^+\rightarrow\frac{5}{2}^+$ rates are extremely strong, $\sim$25 W.u., while the $\frac{11}{2}^+\rightarrow\frac{7}{2}^+$ and $\frac{13}{2}^+\rightarrow\frac{9}{2}^+$ rates are of rather ordinary strength, in qualitative agreement with our discussion assuming that the core-excited admixtures have a large effect on the $E2$ rates. We expect this to be so for several reasons, one of which is that core excitation brings in the participation of protons, which is necessary to obtain large $E2$ rates; i.e., the low-lying 4p-1h ^{43}Ca states are found to be predominantly neutron-hole states.

2. *Resemblance to mass 42*

Flowers and Skouras[55] developed a quite successful understanding of the influence of core excitations on the low-lying $T=0$ and 1 spectra of mass 42. They admixed 2p-0h shell-model states with 4p-2h deformed states with the latter generated in several approximations utilizing a Nilsson[56] representation. The results are quite similar to those discussed in the previous subsection for mass 43. Specifically, for ^{42}Ca the mixing is strongest for $J=2$ and 4 for which the 2p-0h and 4p-2h states are close in energy. The effect of these admixtures on $E2$ rates has been discussed by Flowers and Skouras[55] and by Brown, Arima, and McGrory,[57] who made a comprehensive study of $E2$ effective charges in the $A=16$ and 40 regions. $E2$ rates in a 2p-0h model are much too small; inclusion of 4p-2h admixtures brings the calculated $E2$ rates into much better agreement with the large experimental values, but they still fall short of experiment by a factor of $\sim$2 (Ref. 57). There are several reasons why this might be so. First, inclusion of 4p-2h admixtures may not be adequate. We know from the historic work of Gerace and Green[58] and later studies that higher-order particle-hole admixtures may be important. In addition, it seems reasonable that deformation resulting from the core excitations will enhance the $\Delta N=2$ admixtures not considered here or by Flowers and Skouras.[55] Since the effect of these admixtures is parametrized by effective charges, it seems reasonable that the effective charges derived for the normal states would be too small for these deformed states. This is an area which needs further study.

These considerations should apply to ^{43}Ca as well.

B. Summary

The shell-model predictions and experimental information considered here can be qualitatively understood as follows: The low-lying even-parity $T=\frac{3}{2}$ levels of mass 43 are of highly mixed 4p-1h and 6p-3h character with significant contributions from 8p-5h, etc., quite likely. The admixing gives rise to deformation and to large $E2$ rates. For the $T=\frac{5}{2}$ and high-spin $T=\frac{3}{2}$ even-parity levels, the unperturbed 4p-1h and 6p-3h states are farther apart and the admixtures of core excitations in the yrast states is normal and thus within the domain of an effective shell model. Thus we find generally good agreement of our predictions with experiment for these states.

What of the beta decay matrix elements? They connect the ^{43}K ground state—a normal shell-model state—with ^{43}Ca levels for which we have proposed large core-excited components. Since the GT operator does not connect different $n\hbar\omega$ components, the contributions of the $0\hbar\omega$ and $2\hbar\omega$ components add incoherently and we would expect core excitation might affect the predictions for B_0 by a factor of 2 or less. On the other hand, the first-forbidden operators would connect the 4p-1h ^{43}K ground state with both 3p-0h and 5p-2h ^{43}Ca components and so the contributions add coherently. Thus the effect of core excitations on first-forbidden rates could be considerable. In view of these considerations, the agreement

of the predictions with experiment (Table V) is probably as good as can be expected.

ACKNOWLEDGMENTS

Research was supported by the U.S. Department of Energy under Contract No. DE-AC-02-76-CH00016. Computational work was done on computers of the Lawrence Livermore National Laboratory, Nuclear Chemistry Division. We would like to thank D. J. Millener, who provided the computer program for two-nucleon transfer reactions and for many valuable discussions; B. A. Brown and J. A. Becker for advice, consultation, and computational expertise; and D. R. Manatt for his continued assistance with computer operations.

[1]K. Kubodera, J. Delorme, and M. Rho, Phys. Rev. Lett. **40**, 755 (1978).
[2]I. S. Towner and F. C. Khanna, Nucl. Phys. **A399**, 334 (1983).
[3]D. J. Millener, D. E. Alburger, E. K. Warburton, and D. H. Wilkinson, Phys. Rev. C **26**, 1167 (1982).
[4]D. J. Millener and E. K. Warburton, in *Proceedings of the International Symposium on Nuclear Shell Models,* edited by M. Vallieres and B. H. Wildenthal (World Scientific, Singapore, 1985), p. 365.
[5]I. S. Towner, Annu. Rev. Nucl. Part. Sci. **36**, 115 (1986).
[6]E. K. Warburton, *Interactions and Structures in Nuclei,* edited by R. J. Blin-Stoyle and W. D. Hamilton (Adam Hilger, Bristol, England, 1988), p. 81.
[7]E. K. Warburton, J. A. Becker, B. A. Brown, and D. J. Millener, Ann. Phys. (N.Y.) (in press).
[8]E. K. Warburton, J. A. Becker, D. J. Millener, and B. A. Brown, Brookhaven National Laboratory Report No. 40 890, 1987.
[9]E. K. Warburton and J. A. Becker, Phys. Rev. C **37**, 754 (1988).
[10]P. Endt and C. van der Leun, Nucl. Phys. **A310**, 1 (1978).
[11]T. Lindquist and A. C. G. Mitchell, Phys. Rev. **95**, 444 (1954).
[12]N. Benczer-Koller, A. Schwarzschild, and C. S. Wu, Phys. Rev. **115**, 108 (1959).
[13]C. Chasman, K. W. Jones, and R. A. Ristinen, Phys. Rev. **169**, 911 (1968).
[14]H. W. Taylor, J. D. King, H. Ing, and R. J. Cox, Can. J. Phys. **47**, 1539 (1969).
[15]R. E. Larson and C. H. Gordon, Radiochim. Acta **13**, 61 (1970).
[16]S. L. Waters, Radiochim. Acta **17**, 63 (1971).
[17]Y. Yoshizawa, Y. Iwata, T. Kaku, T. Katoh, J. Ruan, T. Kojima, and Y. Kawada, Nucl. Instrum. Methods **174**, 109 (1980).
[18]R. A. Meyer and T. N. Massey, Lawrence Livermore National Laboratory Report No. CURL-89142, 1983.
[19]J. T. Routti and S. G. Prussin, Nucl. Instrum. Methods **72**, 125 (1969).
[20]A. H. Behbehani, A. M. Al-Naser, A. J. Brown, L. L. Green, A. N. James, C. J. Lister, N. R. F. Rammo, J. F. Sharpey-Schafer, L. H. Zybert, R. Zybert, and P. J. Nolan, J. Phys. G **5**, 1117 (1979).
[21]R. E. Holland and F. J. Lynch, Phys. Rev. C **2**, 1365 (1970).
[22]R. G. Helmer, R. C. Greenwood, and R. J. Gehrke, Nucl. Instrum. Methods **155**, 189 (1978); R. C. Greenwood, R. G. Helmer, and R. J. Gehrke, *ibid.* **159**, 465 (1979), and references quoted therein.
[23]E. K. Warburton and D. E. Alburger, Nucl. Instrum. Methods **A253**, 38 (1986).
[24]G. Wang, E. K. Warburton, and D. E. Alburger, Nucl. Instrum. Methods (to be published).
[25]R. G. Helmer, P. H. M. van Assche, and C. van der Leun, At. Data Nucl. Data Tables **24**, 39 (1979).
[26]The least-squares adjustments were performed using the program GTOL available at the National Nuclear Data Center (BNL).
[27]B. H. Wildenthal, Prog. Part. Nucl. Phys. **11**, 5 (1984).
[28]J. B. McGrory, Phys. Rev. C **8**, 693 (1973).
[29]D. J. Millener and D. Kurath, Nucl. Phys. **A255**, 315 (1975).
[30]B. A. Brown, A. Etchegoyen, W. D. M. Rae, and N. S. Godwin, OXBASH, 1984 (unpublished).
[31]B. A. Brown and B. H. Wildenthal, At. Data Nucl. Data Tables **33**, 347 (1985).
[32]I. S. Towner and F. C. Khanna, Nucl. Phys. **A399**, 334 (1983).
[33]A. Arima, K. Shimizu, W. Bentz, and H. Hyuga, Adv. Nucl. Phys. **18**, 1 (1987).
[34]I. S. Towner, Phys. Rep. **155**, 263 (1987).
[35]B. A. Brown, in *Proceedings of the International Nuclear Physics Conference, Harrogate, United Kingdom 1986,* edited by J. L. Durell, J. M. Irvine, and G. C. Morrison (Institute of Physics, Bristol, 1987), Vol. 2, p. 119.
[36]N. Anyas-Weiss, J. C. Cornell, P. S. Fisher, P. N. Hudson, A. Menchaca-Rocha, D. J. Millener, A. D. Panagiotou, D. K. Scott, D. Strottman, D. M. Brink, B. Buck, P. J. Ellis, and T. Engeland, Phys. Rep. **12**, 201 (1974).
[37]E. Rivet, R. H. Pehl, and B. G. Harvey, Phys. Rev **141**, 1021 (1965).
[38]N. K. Glendenning, Phys. Rev. **137**, B102 (1965).
[39]H. Nann, W. S. Chien, and A. Saha, Nucl. Phys. **A292**, 205 (1979).
[40]T. A. Brody and M. Moshinsky, *Tables of Transformation Brackets* (Monograficisdel Instituto, Mexico, 1960).
[41]I. P. Johnstone, Phys. Rev. C **22**, 2561 (1980).
[42]D. S. Chuu, C. S. Han, S. T. Hsieh, and M. M. King Yen, Phys. Rev. C **27**, 380 (1983).
[43]S. Mordechai, H. T. Fortune, and C. F. Clement, Phys. Rev. C **30**, 507 (1984).
[44]A. Huck, G. Klotz, A. Knipper, C. Miehe, C. Richard- Serre, and G. Walter, Phys. Rev. C **18**, 1803 (1978).
[45]A. H. Behbehani, A. M. Al-Naser, L. L. Green, A. N. James, C. J. Lister, N. R. F. Rammo, J. F. Sharpey-Schafer, H. M. Sheppard, and P. J. Noland, J. Phys. G **5**, 971 (1979).
[46]P. Doll, G. J. Wagner, K. T. Köpfle, and G. Maule, Nucl. Phys. **A263**, 210 (1976).
[47]R. Santo, R. Stock, J. H. Bjerregaard, O. Hansen, O. Nathan, R. Chapman, and S. Hinds, Nucl. Phys. **A118**, 409 (1968); **A139**, 711 (1969).
[48]H. J. Rose and D. M. Brink, Rev. Mod. Phys. **39**, 306 (1967).
[49]A. R. Poletti, E. K. Warburton, J. W. Olness, J. J. Kolata, and Ph. Gorodetzky, Phys. Rev. C **13**, 1180 (1976).
[50]M. Arnold, J. Kowalski, T. Stehlin, F. Träger, and G. zu Putlitz, Z. Phys. A **314**, 303 (1983).
[51]P. J. Ellis and L. Zamick, Ann. Phys. (N.Y.) **55**, 61 (1969).

[52]E. K. Warburton, D. E. Alburger, J. A. Becker, B. A. Brown, and S. Raman, Phys. Rev. C **34**, 1031 (1986).

[53]B. S. Reehal and B. H. Wildenthal, Part. Nucl. Phys. **6**, 137 (1973).

[54]S. T. Hsieh, R. B. M. Mooy, and B. H. Wildenthal, Bull. Am. Phys. Soc. **30**, 731 (1985); S. T. Hsieh, X. Ji, R. Mooy, and B. H. Wildenthal, in *Nuclear Structure at High Spin, Excitation, and Momentum Transfer (McCormick's Creek State Park, Bloomington, Indiana),* Proceedings of the Workshop on Nuclear Structure at High Spin, Excitation and Momentum Transfer, AIP Conf. Proc. No. 142, edited by Hermann Nann (AIP, New York, 1985), p. 357.

[55]B. H. Flowers and L. D. Skouras, Nucl. Phys. **A136**, 353 (1969).

[56]S. C. Nilsson, Mat. Fys. Medd. Dan. Vid. Selsk. **29**, No. 16 (1955).

[57]B. A. Brown, A. Arima, and J. B. McGrory, Nucl. Phys. **A277**, 77 (1977).

[58]W. J. Gerace and A. M. Green, Nucl. Phys. **A123**, 241 (1969).